Predicting the Open-Hole Tensile Strength of Composite Plates Based on Probabilistic Neural Network

Hai-Tao Fan · Hai Wang

Abstract Tensile experiments were performed for open-hole composite plates with three different layups. With the limited number of experimental results, a probabilistic neural network (PNN) based approach is proposed to predict the tensile strength of composite plates with an open-hole. The predictive model takes the geometric parameters, the layup features and the average tensile stress of open-hole composite plates as the inputs and produces the safety status as the intermediate output with the classification function of PNN. Then the critical safety point, that is the open-hole tensile strength, where the safety status turns from survival to failure, is determined with the bi-section searching method. The predictions produce acceptable results whose errors are comparable to the coefficient of variation of experimental results. With experimental data from other studies, further assessments are also made to prove the capability of this model in predicting the open-hole tensile strength of composite plates.

Keywords Open-hole tensile strength · Experimental results · Composite plate · Probabilistic neural network

1 Introduction

Fiber reinforced polymer (FRP) composites are widely used in structural applications owing to its unique features such as the high stiffness, high strength and the potential in tailor-made design. However, composite materials have much more complex failure mechanism compared to that of metal materials [1–3], in particular for the case of composite structures with an open hole. The open-hole effect on the composites, as a classical issue, has been long concerned by many researchers [4–13].

Theoretical methods, such as the fracture mechanics models [5, 6], the progressive damage models [7] and the Continuum damage models [9], were developed to predict the open-hole tensile strength of composite plates. These theoretical models, which are mostly based on the classical mechanics, are very meaningful in finding out the true failure mechanism and

H.-T. Fan · H. Wang (✉)
School of Aeronautics and Astronautics, Shanghai Jiao Tong University, Shanghai 200240, People's
Republic of China
e-mail: wanghai601@sjtu.edu.cn

improving the applications. However, the limitation of knowledge results in more uncertainties when these models are adopted in engineering practice.

Experiments are usually conducted to account for the open-hole effect in engineering practices. Based on characteristic distances determined through experiments, Whitney and Nuismer [4] proposed the point stress criterion and average stress criterion, which are seen as classical methods in the failure prediction of notched structures. However, uncertainties, especially the variability, inevitably exist in experiments. To address this important issue, the experimental results are usually conservatively processed with statistical methods to cover the effect of variability. This makes the experiments costly and time-consuming. In order to reduce the cost of experiments and utilize the experimental results more sufficiently, many researchers have developed various methods for predicting material properties or structural performances based on a limited number of experimental results.

The artificial neural network (ANN), which is a simulation to the nervous system, is often used to make predictions on the properties/behaviors of composites [14–26]. Pidaparti and Palakal [14] developed a back-propagation neural network to predict the non-linear stress–strain behavior of laminates. Labossiere and Turkkan [15] used ANN to predict the failure of composites under plane stress conditions. Lee et al. [16] compared the Tsai-Wu criterion with ANN on the predictive accuracy based on a set of biaxial tests of cross-ply composite tubes made of T300 carbon/epoxy and concluded that ANN showed smaller root-mean-square-error (RMSE). Lee et al. [17] used ANN to predict the fatigue life of carbon/glass fiber reinforced plastic laminates and recognized the effect of the ANN architecture on the prediction. Velten et al. [18] used ANN to predict the wear properties of short-fiber/particle reinforced thermoplastics. Al-Assaf and El Kadi [19] carried out an ANN prediction to get the fatigue life of unidirectional glass fiber/epoxy composites and a satisfactory predictive quality was got with the RMSE less than 20 %. Zhang et al. [20] predicted the storage modulus and damping of short fiber-reinforced composites with ANN. Perera et al. [23] used a back-propagation neural network to predict the ultimate strength of reinforced concrete beams retrofitted in shear by means of externally bonded FRP and further carried out a parametric study with the trained neural network. Camara and Freire [24] developed three types of neural network architectures to model the transverse elasticity modulus of unidirectional composites and got more accurate predictions compared with the Halpin-Tsai mathematical model. Bashir and Ashour [25] modeled the shear strength of FRP- bars-reinforced concrete members with ANN and carried out a parametric study with the trained neural network. Varol et al. [26] used a feed forward back propagation ANN to model the effect of reinforcement properties on the physical and mechanical properties of Al2024-B4C composites and concluded that the well-trained feed forward back propagation ANN model is a powerful tool to predict the effect of reinforcement properties on physical and mechanical properties of composites.

The conventional predicting methods with ANN, whose target is to get the training data fitted as accurately as possible, take the predicted object (e.g. , material properties / structural performances) as certain values. Actually, the experimental results are full of uncertainties, and therefore, the accurate fitting is often meaningless or even makes against finding out the true relationships between the inputs (material properties, structural dimensions and etc.) and outputs (structural performances). For example, for a row of given inputs, the tests may produce different outputs, which is in conflict with the accurate-fitting target of the conventional ANN. Although the conventional ANN based predicting methods pre-select/pre-process the training data before feeding them to the ANN, it is very hard to find out which output is more valid, even with the statistical methods.

The probabilistic neural network (PNN) was designed to make decisions based on probabilistic methods [27, 28], which means PNN can be used to learn from training data with

uncertainties. In this paper, PNN is used to predict the open-hole tensile strength of composite plates based on a limited number of experimental results.

2 Problem Description

Figure 1 shows a composite plate with a central circular hole having diameter D. The plate has length L, width W and thickness h. The volume fraction of 0-ply in the laminate is P_0, while that of 90-ply is P_{90}. The open-hole composite plate is loaded at two ends in the longitudinal direction (direction x) by a uniform distributed tension force σ_t. It is assumed that the composite plate, whose design object is usually the ply stacking sequence, should not fail under the ultimate load at a very high probability.

As we know from the design and manufacturing practice, variability exists both in the material properties and structural parameters. The variability may result from the high porosity caused by insufficient resin flow / vacuum-pumping or inaccurate laying-up. Although the improvement of forming technology of composites, such as the automated prepregs laying-up, has made the variability smaller, it is still a big concern to designers and researchers [29–31].

The open-hole tensile strength of a composite plate, which is related to the material properties and structural parameters, is a value full of uncertainty.

3 Open-Hole Tensile Strength Experiments

Experimental tests were conducted in the Laboratory of Civil Aircraft Structures Testing, Shanghai Jiao Tong University. The layup and the nominal thickness of the laminated test specimens, which are made of T800/Epoxy, are listed in Table 1. The specimens are grouped into TS1, TS2 and TS3 based on their layups. The specimens are named as "TS#-#", where the first "#" represents the group number and the second "#" represents the specimen number in the group. Table 2 shows the typical material properties of T800/Epoxy. All the specimens have a nominal length of 300 mm and a nominal width of 36 mm. The nominal diameter of the circular hole is 5.8 mm. According to the measured data before the tests, obvious variability exists in these geometric parameters.

The experiments were implemented on a SANS CMT5305 300 kN electronic universal testing machine, as shown in Fig. 2. The specimens were fixed on the testing machine and loaded by the increasing displacement at a rate of 2 mm/min until the specimens' breakage makes the axial force decrease. During the loading, the force-displacement curves were recorded. The typical curves of TS1-1, TS2-1 and TS3-1 are shown in Fig. 3. The failure mode of all the test specimens is breakage through the circular hole as shown in Fig. 4. The
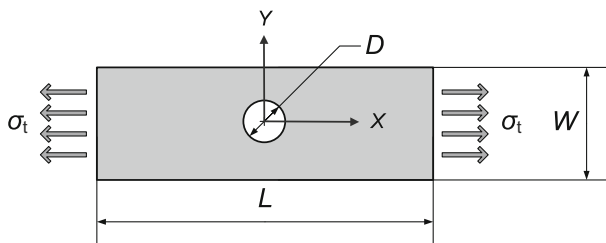

Fig. 1 A composite plate with an open hole subjected to tension

Table 1 T800/Epoxy test specimens

Test specimen group	Lay up	Nominal thickness (mm)	Quantity
TS1	[+45/−45/0/0/+45/−45/90]s	2.632	16
TS2	[+45/−45/0/0/+45/−45/0/0/90]s	3.384	18
TS2	[+45/−45/0/+45/−45/+45/−45/+45/−45/90]s	3.760	18

experimental results are listed in Tables 3, 4, and 5, where "tensile strength" means the maximum end tensile force divided by the cross-section area of the specimen.

4 Modeling

4.1 Probabilistic Neural Network

Probabilistic neural network (PNN), which was proposed by Specht [27, 28], is a special form of radial basis function network. It is mainly suitable for classification problems. The architecture of PNN is shown in Fig. 5. It contains four layers, which are named as the input layer, the pattern layer, the summation layer and the output layer, respectively [27, 28].

The input layer contains one input node for each input attribute. In the pattern layer, there is one neuron for each training instance in the training set, which means the amount of neurons in the pattern layer is equal to that of training instances. Each neuron in the pattern layer has a center point, which is the input vector of the related instance. The pattern layer, together with the summation layer, implements the Parzen windows probability density approximation method [32], in which the conditional probability of class i can be estimated as,

$$g_i(x) = \frac{1}{(2\pi)^{n/2} \prod_{j=1}^{n} \lambda_{ij} N_i} \sum_{r=1}^{N_i} e^{-\sum_{j=1}^{n} \frac{\left(x_j - X_{rj}^i\right)^2}{2\lambda_{ij}^2}} \tag{1}$$

where n is the dimensionality of the input patterns, N_i is the amount of training points belonging to class i, x_j is the j-th input attribute of the input pattern to be classified, X_{rj}^i denotes the j-th input attribute of the r-th training point belonging to class i, λ_{ij} is the smoothing parameter across dimension i of the patterns for the training points belonging to class j. λ_{ij} could

Table 2 Typical material properties of T800/ Epoxy

Property	
Density, ρ (g/mm)	194
Fiber volume fraction, V_f (%)	35 %
Thickness, t (mm)	0.188
Longitudinal modulus, E_{11} (MPa)	157,600
Transverse modulus, E_{22} (MPa)	8,295
Poisson's ratio, μ_{12}	0.32
In-plane shear modulus, G_{12} (MPa)	4,370
Longitudinal tensile strength, X_t (MPa)	2,400
Longitudinal compressive strength, X_c (MPa)	1,400

Fig. 2 The test setup

be adjusted to reflect the significance of each input attribute in the generation of the outputs. The adjustment of λ_{ij} could be seen as an important learning step of the PNN.
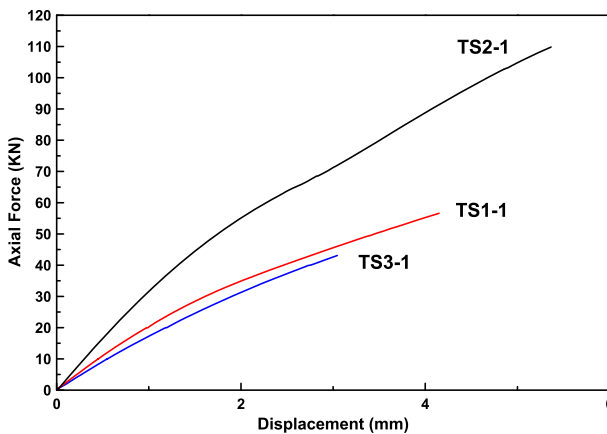

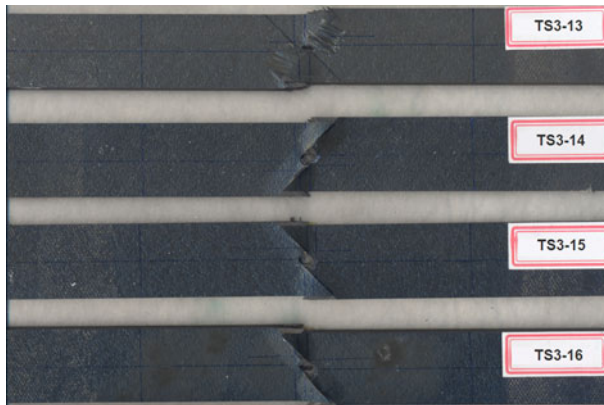**Fig. 3** The typical axial force-displacement curves of test specimens

Fig. 4 The failure mode of test specimens

The output layer implements the category selection by the Bayesian decision criterion. The two-category Bayesian decision criterion can be expressed as follows,

$$\begin{cases} d(x) = \theta_A & if \quad h_A l_A f_A(X) > h_B l_B f_B(X) \\ d(x) = \theta_B & if \quad h_A l_A f_A(X) < h_B l_B f_B(X) \end{cases} \tag{2}$$

where the state can be classified into θ_A and θ_B (e.g., survival and failure). $f_A(X)$ and $f_B(X)$ are respectively the probability density function for category A and B. h_A and h_B are respectively the a priori probability of occurrence of patterns from category A and B. l_A is the loss

Table 3 Experimental results of TS1

Test specimen number	Geometric parameters (mm)				Max load (kN)	Max displacement (mm)	Tensile strength (MPa)
	L	W	h	D			
TS1-1	300.2	36.1	2.61	5.79	56.61	4.15	600.82
TS1-2	300.0	36.0	2.60	5.82	58.27	3.50	622.54
TS1-3	300.0	36.1	2.61	5.82	57.10	4.07	606.02
TS1-4	300.1	36.0	2.60	5.84	59.61	5.23	636.86
TS1-5	300.1	36.0	2.60	5.81	58.16	3.57	621.37
TS1-6	300.1	36.0	2.60	5.81	58.32	3.20	623.08
TS1-7	299.8	36.0	2.60	5.80	58.11	3.47	620.83
TS1-8	300.1	36.0	2.60	5.81	54.07	4.33	577.67
TS1-9	299.8	36.0	2.60	5.80	59.22	4.31	632.69
TS1-10	300.4	36.2	2.61	5.81	61.02	4.35	645.84
TS1-11	300.2	35.8	2.59	5.79	57.62	3.40	621.43
TS1-12	300.1	36.2	2.61	5.81	60.10	3.88	636.10
TS1-13	300.1	36	2.62	5.8	55.56	3.34	589.06
TS1-14	300.1	36	2.61	5.8	58.6	3.24	623.67
TS1-15	300.5	35.9	2.61	5.81	58.04	3.84	619.43
TS1-16	300.1	36	2.6	5.81	57.7	3.37	616.45

Table 4 Experimental results of TS2

Test specimen number	Geometric parameters (mm)				Max load (kN)	Max displacement (mm)	Tensile strength (MPa)
	L	W	h	D			
TS2-1	299.7	36.1	3.47	5.82	109.83	5.37	876.77
TS2-2	300.8	36.6	3.38	5.84	100.04	3.96	808.68
TS2-3	300.4	35.9	3.46	5.84	107.54	5.20	865.76
TS2-4	301.0	36.2	3.41	5.79	101.27	5.21	820.39
TS2-5	300.1	36.1	3.47	5.83	106.22	4.92	847.95
TS2-6	300.2	36.1	3.39	5.83	103.85	4.97	848.59
TS2-7	299.8	36.2	3.50	5.81	108.09	3.75	853.12
TS2-8	300.3	35.9	3.40	5.78	107.73	3.92	882.60
TS2-9	299.8	36.1	3.48	5.82	107.97	6.35	859.44
TS2-10	300	36.0	3.41	5.79	105.06	5.90	855.82
TS2-11	300.2	36.1	3.46	5.83	107.09	5.74	857.36
TS2-12	300.1	36.1	3.39	5.80	96.03	5.49	784.69
TS2-13	300.2	35.8	3.43	5.84	94.11	4.62	766.41
TS2-14	299.5	35.9	3.47	5.80	108.63	6.34	872.02
TS2-15	301.4	36.0	3.44	5.84	110.99	5.93	896.24
TS2-16	300.4	36.0	3.44	5.83	111.47	6.27	900.11
TS2-17	300.8	35.8	3.40	5.86	101.15	4.45	831.01
TS2-18	300.0	36.0	3.43	5.79	107.61	3.93	871.48

associated with the decision $d(x)=\theta_A$ when $\theta=\theta_B$, while l_B is the loss associated with the decision $d(x)=\theta_B$ when $\theta=\theta_A$.

When an input pattern is feed to a trained PNN, the output is produced based on the approximated probability density of different classes. The validity of each training point is reflected in the probability density calculation in an implicit way. PNN often learn more quickly than many neural network models such as back-propagation network, and have had success in the classification field.

4.2 Modeling and Predicting Approach

The geometric parameters (e.g. D, W, h) and layup features (e.g. P_0 and P_{90}) of the open-hole composite plates are assumed to be related to the tensile strength in this paper. The influence of the ply material properties is neglected because the modeling object here is only the open-hole tensile strength of composite plates with the same material. To produce the safety status of the plate, the average axial stress (σ_t) of the plate, together with the above parameters, are taken as the inputs of the PNN. The output of PNN is set to be S, which is equal to 0 or 1 to represent the safety status (1 denotes survival while 0 denotes failure) of the plate.

The flowchart for modeling and predicting the open-hole tensile strength of composite plates may be given as shown in Fig. 6 with details as follows:

1) By using the existing knowledge /experience, the available experimental results are extended to produce the training/testing data. It is also processed to satisfy the input/ output requirement of PNN. As shown in Fig. 7, when we have some open-hole tensile strength experimental results of laminate plates, we can extend them by using the

Table 5 Experimental results of TS3

Test specimen number	Geometric parameters (mm)				Max load (kN)	Max displacement (mm)	Tensile strength (MPa)
	L	W	h	D			
TS3-1	299.9	36.1	3.80	5.86	43.10	3.05	314.19
TS3-2	300.1	36.2	3.78	5.84	45.80	3.22	334.71
TS3-3	299.8	36.0	3.77	5.85	42.56	2.83	313.59
TS3-4	299.8	35.7	3.73	5.84	41.85	4.10	314.28
TS3-5	300.0	35.7	3.74	5.88	42.57	2.88	318.83
TS3-6	300.0	36.0	3.75	5.89	40.87	2.88	302.74
TS3-7	299.8	36.2	3.77	5.87	42.11	3.00	308.56
TS3-8	300.3	36.1	3.75	5.93	42.72	3.36	315.57
TS3-9	300.1	36.2	3.77	5.88	40.80	2.68	298.96
TS3-10	300.5	36.1	3.75	5.92	42.82	3.14	316.31
TS3-11	300.3	35.9	3.74	5.93	41.57	2.74	309.61
TS3-12	300.4	36.1	3.76	5.93	41.83	2.95	308.17
TS3-13	300.0	35.8	3.74	5.89	40.85	3.02	305.10
TS3-14	300.0	35.9	3.74	5.89	42.17	2.99	314.08
TS3-15	300.5	36.1	3.76	5.92	41.30	3.16	304.27
TS3-16	300.3	36.3	3.76	5.93	40.77	3.26	298.71
TS3-17	299.8	36.0	3.75	5.85	41.50	3.14	307.41
TS3-18	300.4	36.2	3.76	5.93	41.24	3.33	302.99

following settings, that is, for a row of experimental results (here means all the experimental results got from one specimen in one successful test), when other parameters are fixed, a) the structure would fail if W decreases, and survive if W increases; b) the structure would fail if D increases, and survive if D decreases; c) the structure would fail if P_0 decreases, and survive if P_0 increases; d) the structure would fail if P_{90} increases, and survive if P_{90} decreases; e) the structure would fail if σ_t increases (to be larger than the experimental tensile strength), and survive if σ_t decreases (to be smaller than the experimental tensile strength).
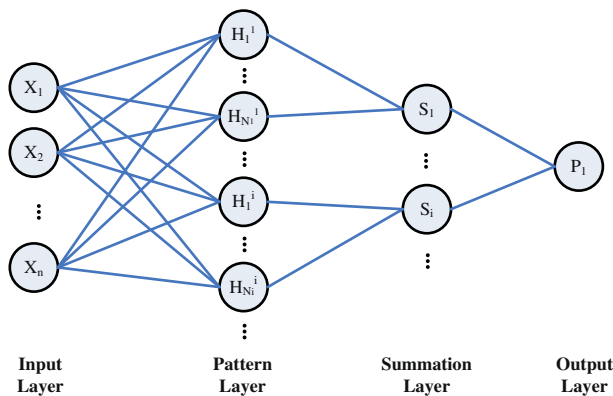

Fig. 5 The architecture of probabilistic neural network

We can also train the PNN with constraints under following three cases. For case (a), the tensile strength of an un-notched ($D=0$ mm) standard ASTM 3039 0-deg unidirectional composite plate ($L=250$ mm, $W=15$ mm, $h=1.0$ mm) is equal to X_t (the longitudinal tensile strength) of a lamina; for case (b), the tensile strength of an un-notched ($D=0$ mm) standard ASTM 3039 90-deg unidirectional composite plate ($L=175$ mm, $W=25$ mm, $h=2.0$ mm) is equal to Y_t (the transverse tensile strength) of a lamina; and for case (c), the tensile strength is zero when $D/W=1$ or $h=0$ or $W=0$. So a set of training/testing data can be derived from each experimental result row by slightly changing the parameter values in the specified spaces.

2) The training data is used to train the PNN. The genetic algorithm optimization is used to train the PNN to get the fittest λ_{ij} corresponding to each input attribute and each class. Each λ_{ij} is encoded into a gene, while a PNN with a series of λ_{ij} is encoded into a chromosome and chromosomes form a population. The population evolves generation by generation to get the optimal combinations of λ_{ij} through the crossover and the mutation operations. The fitness function is set to be the root-mean-square-error (RMSE), which can be expressed as,

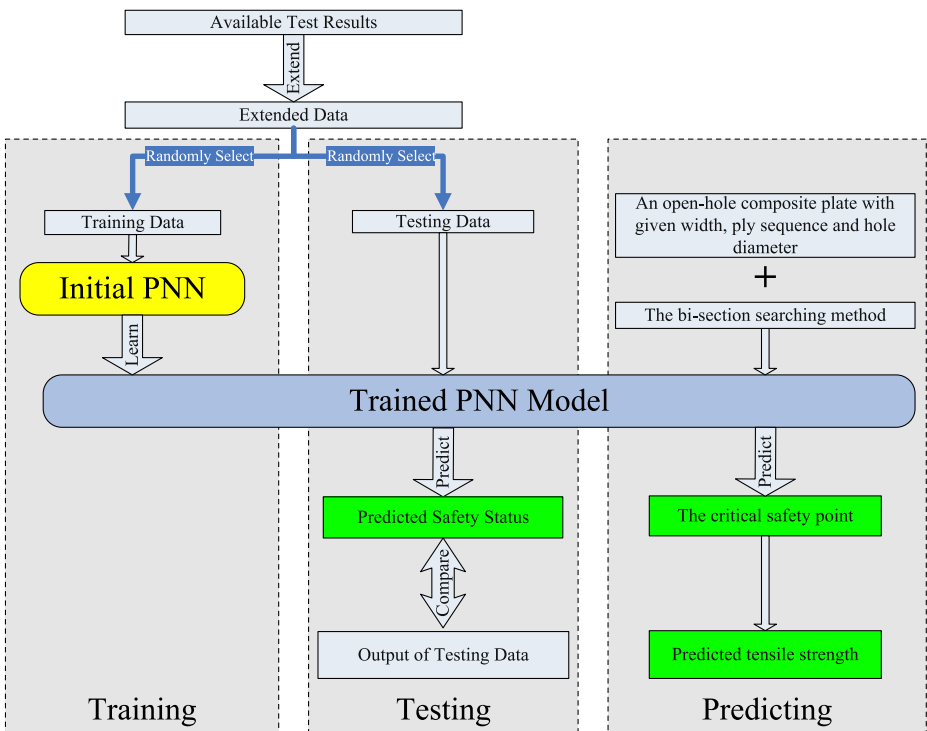$$RMSE = \sqrt{\frac{\sum_{k=1}^{m} \left(Y_k^{pr} \Big/ Y_k^{ex} - 1 \right)^2}{m}} \qquad (3)$$

Fig. 6 The flowchart of the modeling and prediction

Test Specimen Number	Lay up	Geometric Parameters (mm)			Tensile Strength (MPa)
		W	h	D	
TS2-1	[+45/-45/0/0/+45/-45/0/0/90]s	36.1	3.47	5.82	876.77

Lay up	W	h	D	P_0	P_{90}	σ_t	S
[+45/-45/0/0/+45/-45/90]s	36.1	3.47	5.82	0.286	0.143	876.77	Critical
[+45/-45/0/0/+45/-45/90]s	36.1	3.47	5.82	0.286	0.143	↑ 877.53	0
[+45/-45/0/0/+45/-45/90]s	36.1	3.47	5.82	0.286	0.143	↓ 875.12	1
[+45/-45/0/0/+45/-45/90]s	↓ 36.0	3.47	5.82	0.286	0.143	876.77	0
[+45/-45/0/0/+45/-45/90]s	↑ 36.2	3.47	5.82	0.286	0.143	876.77	1
[+45/-45/0/0/+45/-45/90]s	36.1	3.47	↑ 5.84	0.286	0.143	876.77	0
[+45/-45/0/0/+45/-45/90]s	36.1	3.47	↕ 5.82	0.286	0.143	876.77	1
[+45/-45/0/0/90/90/90]s	36.1	3.47	5.82	0.286	↑ 0.429	876.77	0
[+45/-45/0/0/0/0/90]s	36.1	3.47	5.82	↑ 0.571	0.143	876.77	1
[+45/-45/0/0/+45/-45/0]s	36.1	3.47	5.82	↑ 0.429	↓ 0	876.77	1
[+45/-45/0/+45/-45/90]s	36.1	↓ 2.97	5.82	↓ 0.167	↑ 0.167	876.77	0
[+45/-45/0/0/0/+45/-45/90]s	36.1	↑ 3.97	5.82	↑ 0.375	↓ 0.125	876.77	1

Fig. 7 Schematic of training/testing data generation

where Y_k^{pr} is the k-th predicted value , Y_k^{ex} is the k-th experimental value and m is the amount of predictions. The evolution of the population terminates when RMSE becomes smaller than a specified value.

3) The testing data are used to test the PNN.
4) After the training and testing, the PNN model can be adopted to predict the safety status of notched composite plates with different D, W, h, P_0 , P_{90} and σ_t.
5) For an open-hole composite plate with given W, h, D, P_0 and P_{90}, a critical safety points, where the safety status S turns from 1 (survival) to 0 (failure), can be determined through the PNN model. This is an important step that transforms the safety-status classification problem back to a tensile-strength-prediction problem.

Here we set the allowable error (%) in the prediction of the tensile strength to be E_A. We use the following expression to represent the output of the trained PNN model,

$$S = PNN(W, h, D, P_0, P_{90}, \sigma_t) \tag{4}$$

By finding the root (σ_{max} as the unknown tensile strength) of the following equations, we can get the tensile strength predicted.

$$\begin{cases} PNN(W, h, D, P_0, P_{90}, \sigma_{max}) = 1 \\ PNN(W, h, D, P_0, P_{90}, \sigma_{max}(1 + E_A)) = 0 \end{cases} \tag{5}$$

Here the bi-section searching method is used to find the root.

5 Predictions

5.1 Implementation

In the first example, experimental results from TS1, TS2 and TS3 are extended and processed to produce the training/testing data of the predictive model. As shown in Fig. 7, a set of training/testing data can be derived from each experimental result row through the following procedures:

1) To generate a set of parameters (D, W, h, P_0, P_{90}, σ_t) corresponding to different safety status. It is expected that W, h and P_0 will be decreased, while D, P_{90} and σ_t will be increased for the failure status. In contrast, W, h and P_0 will be increased, while D, P_{90} and σ_t will be decreased for the survival status.
2) To select the generated parameter values corresponding to each specified safety status randomly to form rows of training/testing data.
3) Repeat steps 1) and 2) to get a new set of training/testing data.

The training data obtained is then used to train the PNN. After about 10,000 generations of evolution (with a population of 100) with the genetic optimization, the learning of PNN is finished. The testing data obtained is then used to test the predictive accuracy of the PNN. It is found that the trained PNN produces 20,779 correct results when tested with 20,800 rows of testing data. The percentage of wrong classifications is about 0.11 %.

The tested PNN can be used to predict the open-hole tensile strengths of composite plates through the bi-section root finding method, in which E_A is set to be 0.1 %.

5.2 Results and Discussion

As shown in Table 6, the open-hole tensile strengths of test specimens in group TS1 are predicted with the PNN model, which is trained by experimental results of TS2 and TS3. Similarly, the tensile strengths of test specimens in group TS2 and TS3 are also predicted.

Although there is obvious variability in the experimental results, the proposed PNN model shows acceptable predictive accuracy, for which the predictive errors are within ±4%.

The accuracy of the proposed PNN model is also evaluated through the predictions on the open-hole tensile strength of composite plates by using existing experimental data [33, 34]. Each prediction is made based on all the other experimental results of open-hole composite plates with the same material. The prediction results for the second example are listed in

Table 6 Predicted open-hole tensile strengths of test specimens

Test specimens	Open-hole tensile strength (MPa)		Error[a] (%)
	Experimental[b]	Predicted[c]	
TS1	618.4 (2.86 %)[d]	598.2	−3.27
TS2	849.9 (4.23 %)	880.0	3.54
TS3	310.4 (2.75 %)	314.8	1.42

[a] Error=100 % (predicted/experimental−1)

[b] The average experimental tensile strength

[c] Predicted with the PNN model trained by the other two groups of experimental data

[d] The coefficient of variation

Table 7. It should be noted that the experimental data from Ref. [33] has been transformed back to the open-hole tensile strength of composite plates with a finite width. It can be seen that the maximum error is about −8.49 % which is greater than that in Table 6. This is probably because the amount of experimental results used in each prediction in Table 6 is 34/36, which is greater than13/16 in the second example. On the other hand, for experimental results in Table 6, there is only manufacturing variability in some geometric parameters of test specimens, while in the second example, the geometric parameters of test specimens vary in a much larger range, which makes the predictions harder.

Table 7 Predicted open-hole tensile strengths of test specimens based on experimental data from references

Reference	Material	Lay up	Geometric parameters (mm)		Open-hole tensile strength (MPa)		Error[a] (%)
			D	W	Experimental	Predicted[b]	
Tan [33]	AS4/3502	[0/90/±45]$_s$	0	12.7	695.1	713.4	2.63
			0.46	12.7	648.9	648.1	−0.12
			2.54	12.7	435.7	401.9	−7.76
			6.35	25.4	349.0	374.4	7.28
			7.62	25.4	325.0	339.7	4.52
			10.41	34.8	311.9	298.7	−4.23
			15.49	47.5	271.3	290.6	7.11
		[0/90/90/0]$_s$	0	12.7	975.0	1046.3	7.31
			0.46	12.7	984.6	925.2	−6.03
			2.54	12.7	713.3	750.2	5.17
			6.35	25.4	569.5	544.4	−4.41
			7.62	25.4	441.4	470.4	−6.57
			15.49	47.5	510.1	466.8	−8.49
Afaghi-Khatibi et al. [34]	AS4/Epoxy	[0/90]$_{4s}$	6	30.0	535.6	504.1	−5.88
			10	30.0	416.0	428.6	3.03
			20	30.0	202.6	195.0	−3.75
			10	83.6	448.2	434.5	−3.06
			18	82.1	316.7	335.5	5.94
			20	83.1	310.1	317.8	2.48
			30	82.8	252.2	246.9	−2.10
			60	83.8	138.1	129.6	−6.15
		[0/±45/90]$_{2s}$	6	30.0	334.0	350.0	4.79
			10	30.0	320.9	334.7	4.30
			15	30.0	209.8	211.3	0.71
			20	30.0	126.0	119.4	−5.24
			12	60.0	338.0	351.2	3.91
			20	60.0	291.0	299.5	2.92
			30	60.0	188.7	178.4	−5.46
			40	60.0	137.4	127.9	−6.91

[a] Error=100 % (predicted/experimental−1)

[b] Predicted with the PNN model trained by all the other experimental results of open-hole composite plates with the same material

Generally, predictions show that the proposed model is capable of predicting the open-hole tensile strength of composite plates based on a limited number of experimental results with acceptable accuracy. However, compared with the existing theoretical models, the limitation of this model is that it can only predict the open-hole tensile strength of composite plates with the same material and its predictive ability is highly restricted by the test matrix. It is also should be noted that in the calculations, the convergence of the PNN optimization usually needs lots of hours on a PC and the stochastic process in the genetic optimization method makes the calculation time hardly to be estimated.

6 Conclusion

In this paper a PNN based approach has been proposed to predict the open-hole tensile strength of composite plates based on a limited number of experimental results. As a probabilistic method, the PNN can avoid the over-fitting of experimental data. The key issue of this approach is to utilize the limited experimental results and existing knowledge sufficiently by converting the strength prediction problem into a classification problem. To evaluate the predictive accuracy, predictions were implemented based on three sets of open-hole tensile strength tests of composite plates. Further assessments are also made with experimental data from other studies. Compared with the variability commonly existing in the experimental data, the PNN model produces acceptable predictions. It also shows that the proposed model can make predictions based on limited test data without any pre-selection. We believe that the proposed model could be extended to make predictions on other performances of composite structures when there is obvious variability in the observed values for the predicted indices.

References

1. Waddoups, M.E., Eisenmann, J., Kaminski, B.E.: Macroscopic fracture mechanics of advanced composite materials. J. Compos. Mater. **5**(4), 446–454 (1971)
2. Beaumont, P.: The failure of fibre composites: an overview. J. Strain Anal. Eng. **24**(4), 189–205 (1989)
3. Puck, A., Schürmann, H.: Failure analysis of FRP laminates by means of physically based phenomenological models. Compos. Sci. Technol. **58**(7), 1045–1067 (1998)
4. Whitney, J., Nuismer, R.: Stress fracture criteria for laminated composites containing stress concentrations. J. Compos. Mater. **8**(3), 253–265 (1974)
5. Backlund, J., Aronsson, C.G.: Tensile fracture of laminates with holes. J. Compos. Mater. **20**(3), 259–286 (1986)
6. Tan, S.: Laminated composites containing an elliptical opening. I. Approximate stress analyses and fracture models. J. Compos. Mater. **21**(10), 925–948 (1987)
7. Nguyen, B.N.: Three-dimensional modeling of damage in laminated composites containing a central hole. J. Compos. Mater. **31**(17), 1672–1693 (1997)
8. Morais, A.B..: Open-hole tensile strength of quasi-isotropic laminates. Compos. Sci. Technol. **60**(10), 1997–2004 (2000)
9. Maa, R.H., Cheng, J.H.: A CDM-based failure model for predicting strength of notched composite laminates. Compos. B Eng. **33**(6), 479–489 (2002)
10. Green, B., Wisnom, M., Hallett, S.: An experimental investigation into the tensile strength scaling of notched composites. Compos. A Appl. Sci. **38**(3), 867–878 (2007)
11. Ghezzo, F., Giannini, G., Cesari, F., Caligiana, G.: Numerical and experimental analysis of the interaction between two notches in carbon fibre laminates. Compos. Sci. Technol. **68**(3), 1057–1072 (2008)
12. O'Higgins, R., McCarthy, M., McCarthy, C.: Comparison of open hole tension characteristics of high strength glass and carbon fibre-reinforced composite materials. Compos. Sci. Technol. **6**(13), 2770–2778 (2008)
13. Flatscher, T., Wolfahrt, M., Pinter, G., Pettermann, H.: Simulations and experiments of open hole tension tests—assessment of intra-ply plasticity, damage, and localization. Compos. Sci. Technol. **72**(10), 1090–1095 (2012)

14. Pidaparti, R., Palakal, M.: Material model for composites using neural networks. AIAA J. **31**(8), 1533–1535 (1993)
15. Labossiere, P., Turkkan, N.: Failure prediction of fibre-reinforced materials with neural networks. J. Reinf. Plast. Compos. **12**(12), 1270–1280 (1993)
16. Lee, C., Hwang, W., Park, H., Han, K.: Failure of carbon/epoxy composite tubes under combined axial and torsional loading 1. Experimental results and prediction of biaxial strength by the use of neural networks. Compos. Sci. Technol. **59**(12), 1779–1788 (1999)
17. Lee, J., Almond, D., Harris, B.: The use of neural networks for the prediction of fatigue lives of composite materials. Compos. A Appl. Sci. **30**(10), 1159–1169 (1999)
18. Velten, K., Reinicke, R., Friedrich, K.: Wear volume prediction with artificial neural networks. Tribol. Int. **33**(10), 731–736 (2000)
19. Al-Assaf, Y., El Kadi, H.: Fatigue life prediction of unidirectional glass fiber/epoxy composite laminae using neural networks. Compos. Struct. **53**(1), 65–71 (2001)
20. Zhang, Z., Friedrich, K., Velten, K.: Prediction on tribological properties of short fibre composites using artificial neural networks. Wear **252**(7), 668–675 (2002)
21. Zhang, Z., Friedrich, K.: Artificial neural networks applied to polymer composites: a review. Compos. Sci. Technol. **63**(14), 2029–2044 (2003)
22. Kadi, H.E.: Modeling the mechanical behavior of fiber-reinforced polymeric composite materials using artificial neural networks—a review. Compos. Struct. **73**(1), 1–23 (2006)
23. Perera, R., Barchin, M., Arteaga, A., Diego, A.D.: Prediction of the ultimate strength of reinforced concrete beams FRP-strengthened in shear using neural networks. Compos. B Eng. **41**(4), 287–298 (2010)
24. Camara, E.C.B., Freire, R.C.S.: Using neural networks to modeling the transverse elasticity modulus of unidirectional composites. Compos. B Eng. **42**(7), 2024–2029 (2011)
25. Bashir, R., Ashour, A.: Neural network modelling for shear strength of concrete members reinforced with FRP bars. Compos. B Eng. **43**(8), 3198–3207 (2012)
26. Varol, T., Canakci, A., Ozsahin, S.: Artificial neural network modeling to effect of reinforcement properties on the physical and mechanical properties of Al2024-B4C composites produced by powder metallurgy. Compos. B Eng. **54**, 224–233 (2013)
27. Specht, D.F.: Probabilistic neural networks. Neural Netw. **3**(1), 109–118 (1990)
28. Specht, D.F.: Enhancements to probabilistic neural networks. In: Proceedings of the IEEE International Joint Conference on, Neural Networks, pp. 761–768 (1992)
29. Noor, A.K., Starnes, J.H., Peters, J.M.: Uncertainty analysis of composite structures. Comput. Methods Appl. Mech. **185**(2), 413–432 (2000)
30. Manan, A., Cooper, J.: Design of composite wings including uncertainties: a probabilistic approach. J. Aircr. **46**(2), 601–607 (2009)
31. Sriramula, S., Chryssanthopoulos, M.K.: Quantification of uncertainty modelling in stochastic analysis of FRP composites. Compos. A Appl. Sci. **40**(11), 1673–1684 (2009)
32. Parzen, E.: On estimation of a probability density function and mode. Ann. Math. Stat. **33**(3), 1065–1076 (1962)
33. Tan, S.C.: Laminated composites containing an elliptical opening. II Experiment and model verification. J. Compos. Mater. **21**(10), 949–968 (1987)
34. Afaghi-Khatibi, A., Ye, L., Mai, Y.: An effective crack growth for residual strength evaluation of composite laminates with circular holes. J. Compos. Mater. **30**(2), 142–163 (1996)